Journal of Applied Chemical Research, 8, 4, 123-142 (2014)

Journal of Applied Chemical Research

www.jacr.kiau.ac.ir

The Kinetic and Thermodynamic Study for Decolorization of Congo red from Aqueous Solution Using Electrocoagulation Process

Neamat Mohammadlou, Mohammad Hasan Rasoulifard*, Motreaz Vahedpour
Mohamad Reza Eskandarian
Department of Chemistry, Faculty of Sciences, University of Zanjan, Zanjan, Iran

Received 16 Jun 2014; Final version received 17 Sep. 2014

Abstract

The removal of color from synthetic wastewater containing Congo red was experimentally investigated using electrocoagulation process. The effects of operational parameters such as current density, electrolysis time, electrolyte concentration, electrode distance, initial dye concentration, initial pH and temperature on color removal efficiency were investigated in this study. The tentative results showed that Congo red in the aqueous phase was removed effectively by electrocagulation procedure. Optimum operating range for each of these operating variables was experimentally determined. Under the conditions of an initial dye concentration of 50mg/l, electrolysis time 5min, initial pH 7.5, current density 150A/m^2, sodium chloride concentration 10g/l, interelectrode distance 0.5 cm, the color removal efficiency reached 98% when electrical energy consumption in this conditions for the decolorization of the dye solution containing Congo red was 0.46 KWh/m^3. Outcomes showed that the first-order rate equation could be described correlation for the decolorization rate of Congo red. The thermodynamic parameters, such as ΔH^o, ΔS^o and ΔG^o, were also determined and evaluated. Further the experimental data were tested with different adsorption isotherm model to describe the electrocoagulation process.

Keywords: *Electrocoagulation, Wastewater, Decolorization, Congo Red, Thermodynamic and kinetic.*

Introduction

Many industries use dyes and pigments to colourize their products. Some dyes with concentrations that they are discharged to the environment, are often nonpoisonous, however, they give undesirable perspective

---

***Corresponding author:** *Mohammad Hasan Rasoulifard, Department of Chemistry, Faculty of Sciences, University of Zanjan, Zanjan, Iran Email: m_h_rasoulifard@znu.ac.ir, Tel.: +98 2415152591, Fax: +98 241 5152477.*

to the water streams [1], whereas, some other dyes are poisonous and carcinogen and cause sever toxicity for aqueous microorganisms [2]. Dyes also can prevent from photosynthesis in aqueous ecosystems by absorbing sunlight. Sulfur dyes can rapidly reduce oxygen content of the water and so, are harmful to aqueous organisms [3]. Therefore, it is necessary to find an effective method of wastewater treatment in order to remove them from textile effluents.

A large range of physico-chemical processes have been proposed :coagulation with alum, ferric chloride, magnesium chloride and lime or polymers [4], adsorption on activated carbon, polymer and mineral sorbents or biosorbents[5,6] chemical oxidation [7,8] photolysis [9] photocatalytic degradation[10-12]suspended [13,14] or supported photocatalysis [15] and electrophotocatalysis [16].

In this work we used an electrocoagulation because more effective and rapid organic matter separation than in coagulation; the amount of chemicals required is small; the operating costs are much lower than in most conventional technologies [17].

EC technique uses a direct current source between metal electrodes immersed in polluted water. The electrical current causes the dissolution of metal electrodes commonly iron or aluminum into wastewater. The metal ions, at an appropriate pH, can form wide ranges of coagulated species and metal hydroxides that destabilize and aggregate the suspended particles or precipitate and adsorb dissolved contaminants [18].

The mechanism of removal of pollutants by EC process using iron electrodes can be explained as follows [19]. Iron upon oxidation in an electrolytic system produces iron hydroxide, $Fe(OH)_n$ where n = 2 or 3. Two mechanisms have been proposed for the production of $Fe(OH)_n$.

Mechanism 1:

Anode:

$$4Fe_{(s)} \rightarrow 4Fe_{(aq)}^{2+} + 8e^{-} \quad (1)$$

$$4\,Fe_{(aq)}^{2+} + 10\,H_2O_{(l)} + O_{2(g)} \rightarrow 4Fe(OH)_{3(s)} + 8H_{(aq)}^{+} \quad (2)$$

Cathode:

$$8H_{(aq)}^{+} + 8e^{-} \rightarrow 4H_{2(g)} \quad (3)$$

Overall:

$$4\,Fe_{(s)} + 10\,H_2O_{(l)} + O_{2(g)} \rightarrow 4Fe(OH)_{3(s)} + 4H_{2(g)} \quad (4)$$

Mechanism 2:

Anode:

$$Fe_{(s)} \rightarrow Fe_{(aq}^{)2+} + 2\,e^{-} \quad (5)$$

$$Fe_{(aq)}^{2+} + 2\,OH_{(aq)}^{-} \rightarrow Fe(OH)_{2(s)} \quad (6)$$

Cathode:

$$2H_2O_{(l)} + 2\,e^{-} \rightarrow H_{2(g)} + 2\,OH_{(aq)}^{-} \quad (7)$$

Overall:

$$Fe_{(s)} + 2\,H_2O_{(l)} \rightarrow Fe(OH)_{2(s)} + H_{2(g)} \quad (8)$$

The insoluble metal hydroxides of iron can remove dye molecules by surface complexation or electrostatic attraction. In surface complexation, it is assumed that the dye molecule can act as a ligand to bind a hydrous iron moiety with precipitation and adsorption mechanisms [20-24]:

$$\text{Precipitation: }\begin{cases}\text{DYE+ monomeric Fe} \longrightarrow [\text{DYE-monomeric Fe}]_{(s)} & (9)\\[2ex] \text{DYE+ Polymeric Fe} \longrightarrow [\text{DYE-Polymeric Fe}]_{(s)} & (10)\end{cases}$$

$$\text{Adsorption: }\begin{cases}\text{DYE+ Fe(OH)}_{3\,(S)} \longrightarrow [\text{Sludge}] & (11)\\[2ex] [\text{DYE- Polymeric Fe}]_{(S)} + \text{Fe(OH)}_{3\,(S)} \longrightarrow [\text{Sludge}] & (12)\end{cases}$$

The thermodynamic parameters of the adsorption process were determined from the experimental data obtained at various temperatures using the equations [25, 26]:

$$K_d = q_e / C_e \tag{13}$$

$$LnK_d = -\frac{\Delta G^\circ}{RT} = \frac{\Delta S^\circ}{R} - \frac{\Delta H^\circ}{RT} \tag{14}$$

$$\Delta G = \Delta H - T\Delta S \tag{15}$$

where K_d is the distribution coefficient for the adsorption, q_e is the amount of dye (mmol) adsorbed on the adsorbent per l of solution at equilibrium, C_e is the equilibrium concentration (mmol/l) of the dye in solution, T is the absolute temperature, R is gas constant, ΔG^o, ΔH^o, and ΔS^o are Gibbs free energy change, enthalpy change and entropy change, respectively. The values of enthalpy change (ΔHo) and entropy change (ΔSo) are obtained from the slope and intercept of lnKd versus 1/T plots, which are calculated by a curve fitting program.

Congo red (CR) or 1-naphthalenesulfonic acid, 3,3′-(4,4′-biphenylenebis (azo)) bis (4-amino-) disodium salt is a benzidine-based anionic diazo dye prepared by coupling tetrazotised benzidine with two molecules of napthionic acid (Table 1).

Table 1. Structure of C.I. Congo Red.

Chemical structure	Color index number	λ_{max} (nm)	Chemical Class	M_W ($gmol^{-1}$)
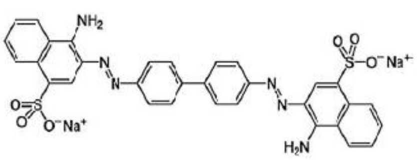	22120	497	Diazo	696.7

This anionic dye can be metabolised to benzidine, a known human carcinogen. Effluent containing Congo red is largely produced from textiles, printing, dyeing, paper, and plastic industries etc. The treatment of contaminated Congo red in wastewater is not straightforward, since the dye is generally present in sodium salt form giving it very good water solubility. Also, the high stability of its structure makes it difficult to biodegrade and photodegrade [27]. In this study electrocoagulation were tested to removal of Congo red from wastewater to investigation of the effect of operational parameters and kinetics and thermodynamic study.

Experimental

Materials and Methods

The batch experimental cell is shown in Figure 1.

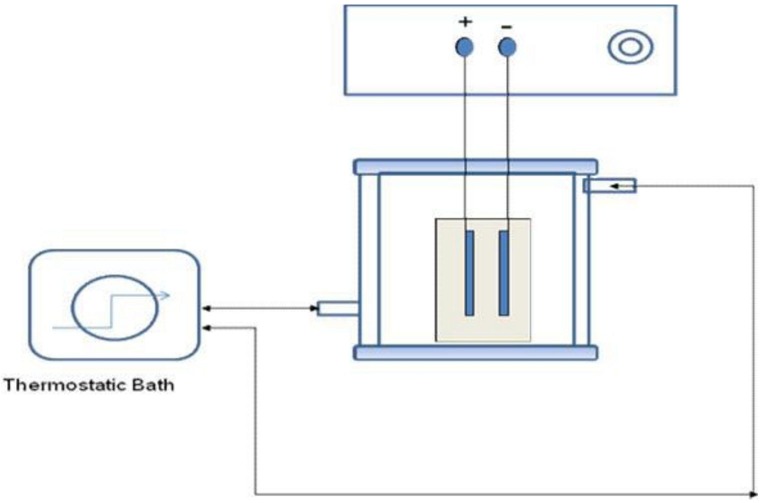

Figure 1. Schematic representation of the electrocoagulation cell.

The conductivity of solutions was raised up and adjusted in different values by the addition of NaCl (Fluka, Switzerland). The pH of the solutions was measured by pH meter (Metrohm 654, Switzerland) and adjusted by adding NaOH or HCl (Merck, Germany) solutions. Iron plates were used as anode and steel plates were used as cathode. Dimensions of electrodes were 30mm×20mm×2mm so, total areas (*A*) of these were 4.4×10^{-4} m^2 and the distance between two electrodes in EC cell was 10mm in all experiments. The electrodes were connected to a DC power supply (APS-133, Iran) with galvanostatic operational options for controlling the current density. The current density (CD) was calculated through the equation as follows:

$$CD = I(A)/2S_{electrode}(m^2) \tag{16}$$

Where I is the current (A) and S is surface area of the electrode (m^2).

In each run, 50 ml of the dye solution was decanted into the electrolytic cell. At the end of electrocoagulation, all samples were allowed to settle for 20 min in a 50 ml vessel before any analysis. Neither centrifuging nor filtration was performed.

Chemical analysis

The dye concentrations were determined from their absorbance characteristics in the UV-vis range (200–800 nm) with the calibration method. For these measurements, the maximum adsorption (λ_{max}) wavelength of dyes was determined by measuring their absorbance at various wavelengths (Table 1). The calculation of color removal efficiency after electrocoagulation treatment was performed using this formula:

$$R\,(\%) = \frac{C_o - C}{C_o} \times 100 \qquad (17)$$

Where C_0 and C are concentrations of dye before and after electrocoagulation in mg l_{-1}, respectively Electrical energy consumption and current efficiency are very important economical parameters in EC process like all other electrolytic processes. Electrical energy consumption per volume of treated effluent (Wh m^{-3}) was also calculated using the Eq. 18:

$$E = VIt/\,V_S \qquad (18)$$

Where I is the average applied current (A), V is the average cell voltage (V), t is the electrolysis time (h), Vs is the solution volume (m3).

Results and Discussion

Effect of current density on the efficiency of color removal and energy consumption

In all electrochemical processes, current density is the most important parameter for controlling the reaction rate within the reactor. It is well known that the amount of current density determines the coagulant production rate, and adjusts the rate and size of the bubble production, and hence affects the growth of flocks [28, 29].

The amount of electrode material dissolved or consumed during the electrocoagulation process depends heavily on the current density as described by the faraday's law.

$$C = \frac{MIt}{ZFV} \qquad (19)$$

Where, C is the concentration of iron ions (g/l); M is the molecular weight (g/mol); I is the current (A); t is time (S); Z is the number of electrons involved in the redox reaction; and F is the faraday's constant.

To investigate the effect of current density on the efficiency of color removal, electrocoagulation process was carried out using various current densities. Fig. 2 shows the color removal percentage and electrical energy consumption against current density applied to the electrodes in the EC process.

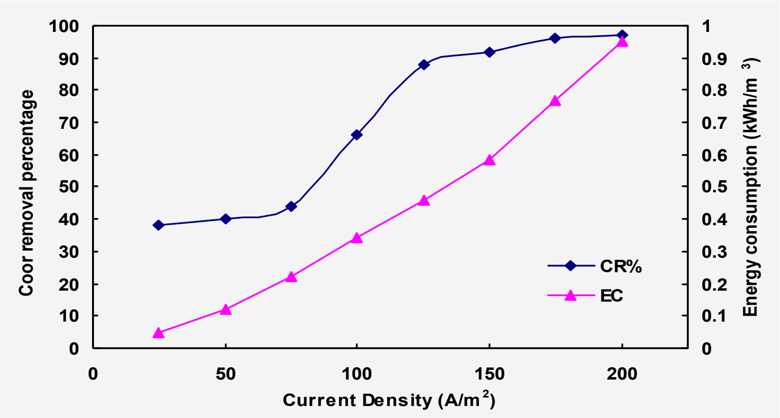

Figure 2. Effect of current density on the efficiency of color removal and energy consumption (C.D = 150 A/m^2, d = 1cm, [NaCl] = 10 g/l, A = 4.4×10 $^{-4}$ m^2, [Congo red] = 50ppm, pH $_i$= 6.7, V$_S$= 50ml).

Raising current density causes a corresponding increase in the oxidized iron production from electrodes and electrical energy consumption increase because base on the equation 18, the current (I) and Voltas (V) increase. The optimum current density of 150Am−2 was used for the color removal from dye solution containing Congo red.

Effect of time of electrolysis on the efficiency of color removal and energy consumption

Reactive time also influences the treatment efficiency of the electrochemical process. Electrolysis time (t) determines the production rate of Fe^{2+} or Fe^{3+} ions from iron electrodes. Figure 3 shows the relationship between the color removal efficiency and electrical energy consumption against the electrolysis time. The color removal efficiency depends directly on the concentration of hydroxyl and metal ions produced on the electrodes and electrical energy consumption depends directly on the time of electrolysis following in Eq. 18. Therefore, according to the results showed in Figure 3, the optimum electrolysis time was 5 min for the color removal from Congo red dye solutions.

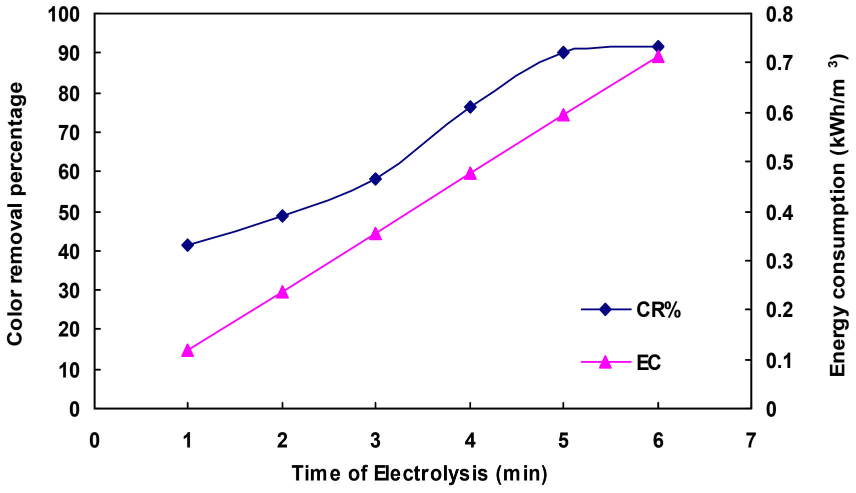

Figure 3. Effect of time of electrolysis on the efficiency of color removal and energy consumption (C.D = 150 A/m^2 , d = 1cm , [NaCl] = 10 g/l , A = 4.4×10 $^{-4}$ m^2, [Congo red] = 50ppm, pH $_i$= 6.7, V$_S$= 50ml).

Effect of the electrolyte concentration on the efficiency of color removal and energy consumption

Table salt is usually employed to increase the conductivity of the water or wastewater to be treated. Solution conductivity affects the current efficiency, cell voltage and consumption of electrical energy in electrolytic cells. Conductivity of dye solutions was adjusted using NaCl in the range of 1–20 mgl^{-1} and the EC process treated these dye solutions. The percentage of color removal and energy consumption was measured as a function of electrolyte concentration in solution. It was found that with the addition of more NaCl to the dye solutions, the color removal rate increased slightly. Probably this process occur because the Na$^+$ and Cl$^-$ ions make cover solution around the dye and adsorbent molecules and lead to increase collision between them and increase color removal percentage.

Increasing electrolyte concentration in solution resulted in the reduction of cell voltages that caused a decrease in electrical energy consumption.

These results have been shown for Congo red in Figure 4. NaCl concentration in all the experimental exceed to 10 mgl^{-1} due high color removal percentage and low electric energy consumption.

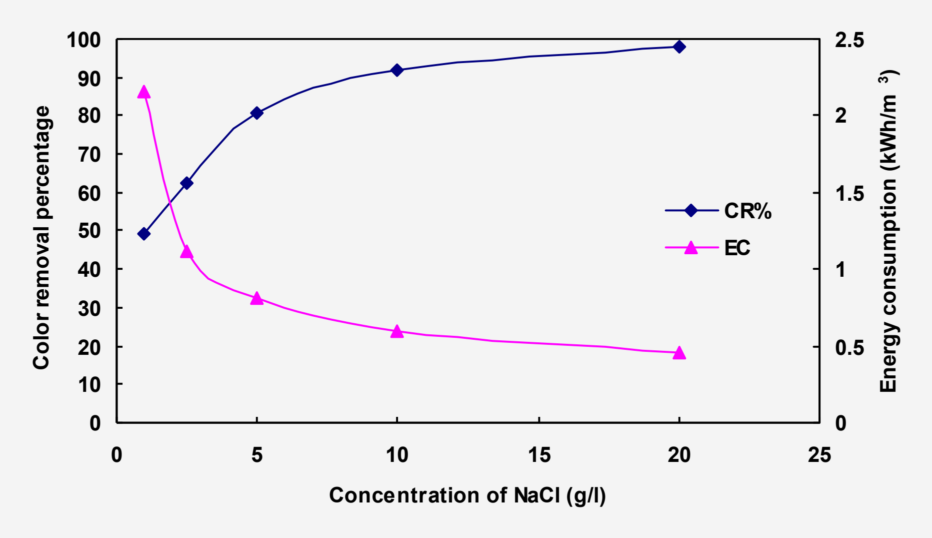

Figure 4. Effect of the electrolyte concentration on the efficiency of color removal and energy consumption (t_{EC} = 5min , C.D = 150 A/m^2 , d = 1cm , A = 4.4×10^{-4} m^2, [Congo red] = 50ppm , pH$_i$= 6.7, V_S= 50ml).

Effect of the distance between electrode on the efficiency of color removal and energy consumption

The effect of interelectrode distance on the removal efficiency and energy consumption was examined at 0.5–2 cm. The effect of interelectrode distance on the color removal efficiency and electrical energy consumption is shown in Figure 5. As it can be seen when the interelectrode distance increases from

0.5 to 1.5 cm, the color removal efficiency decreases slightly. This process may be occur because less space between electrode that make increase condense generated bubble and this process lead to fast removal of iron hydroxide flocks that adsorb dye molecules by flotation.

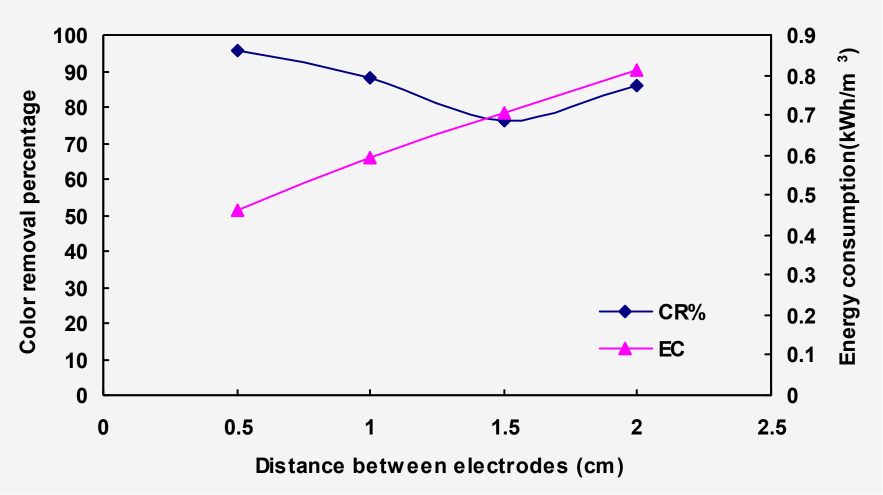

Figure 5. Effect of the distance between electrode on the efficiency of color removal and energy consumption (t_{EC} = 5min , C.D = 150A/m^2, [NaCl] = 10g/l, A = 4.4×10^{-4} m^2, [Congo red] = 50ppm, pH $_i$= 6.7, V_S= 50ml)

When the inter electrode distance increases to 2 cm, the color removal efficiency increases slightly. That is due much space those iron hydroxides motioned and make increase collision between dye and iron hydroxide flocks and lead to increasing adsorption process. Also with increasing distance between electrodes for constant current density, consume Voltas and electrical energy consumption increase. That is due to increase resistance between electrodes with increase solution volume between electrodes. So when the electrode distance is 0.5 cm, could give maximum color removal percentage with less electrical energy consumption.

Effect of initial dye concentration on the efficiency of color removal and decolorization concentration

The dye solutions with different initial concentrations in the range of 10–80 mg l^{-1} were treated by EC in optimized current density and time of electrolysis values. The initial dye concentration was plotted against related color removal percentage and decolorization concentration for Congo red solutions (Figure 6).

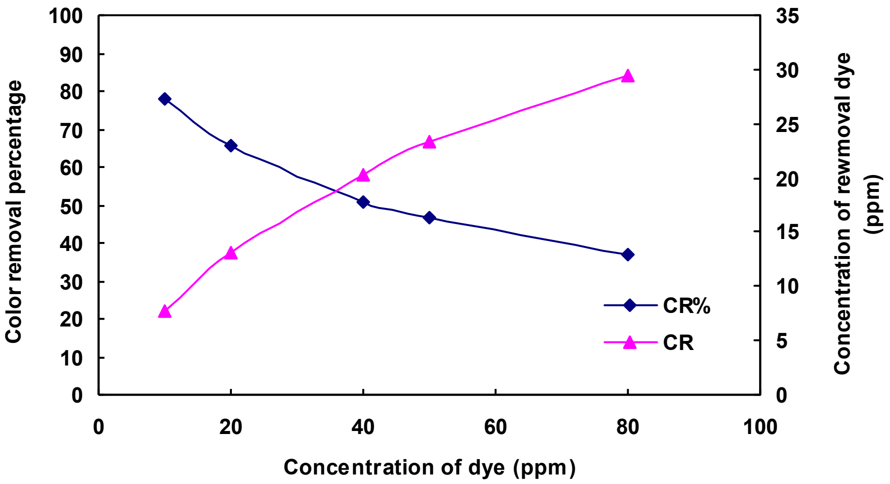

Figure 6. Effect of initial dye concentration on the efficiency of color removal and decolorization capacity (t_{EC} = 5min, C.D =150 A/m^2, d = 1cm, [NaCl] = 10g/l, A = 4.4×10^{-4} m^2, pH $_i$= 6.7, V_S= 50ml).

According to the results, in same condition, with increase initial dye concentration, the amount of removal concentration (mg/l) increase too, but generally, color removal percentage decrease. Then amount of color removal depend on initial dye concentration because effective collision between adsorbent and dye molecules increase and lead to adsorption increase.

However, the increase of initial dye concentration caused a steady increase in decolorization capacity. Kobya et al. [22] and Daneshvar [30] reported similar results for the decolorization of reactive dye solutions by EC process.

Effect of initial pH on the efficiency of color removal and final pH

It has been established that the influent pH is an important parameter influencing the performance of the EC process [30]. To examine its effect, the dye solution was adjusted to the desired pH for each experiment by adding sodium hydroxide or sulfuric acid solution. Color of Congo red transfer in acidic medium then UV-Vis spectrum of this dye at different pH investigated and showed in Figure 7. λ_{max} for Congo red in the acidic medium and under pH=5 changed and go higher wavelength.

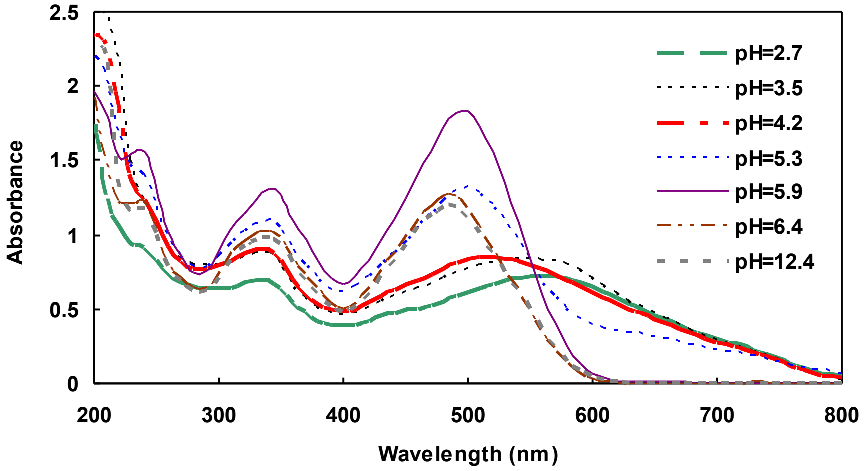

Figure 7. Effect of initial pH on the absorbance of Congo red solution in wavelength 200-800 (t_{EC} = 5min, C. D = 150A/m^2, d = 1cm , [NaCl] = 10g/l , A = 4.4×10 $^{-4}$ m^2,[Congo red] = 50ppm. V_S= 50ml).

The color removal percentages for dye solutions with various initial pH values were shown in Figure 8. The results revealed that when pH of the dye solutions was between 6.5 and 8, there was maximum color removal efficiency. Hence, there is no need for the addition of chemicals to change the initial pH values.

Figure 9 showed that pH of the initial solution has to increase during in the EC process.

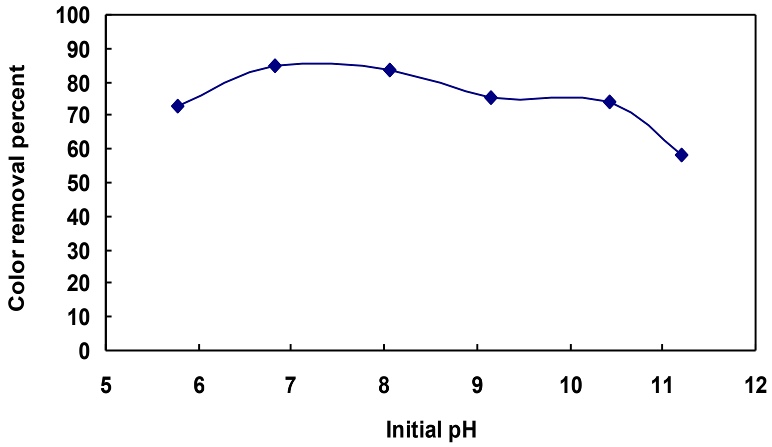

Figure 8. Effect of initial pH on the efficiency of color removal (tEC = 5min, C. D = 150A/m2, d = 1cm , [NaCl] = 10g/l , A = 4.4×10 -4 m2,[Congo red] = 50ppm, VS= 50ml).

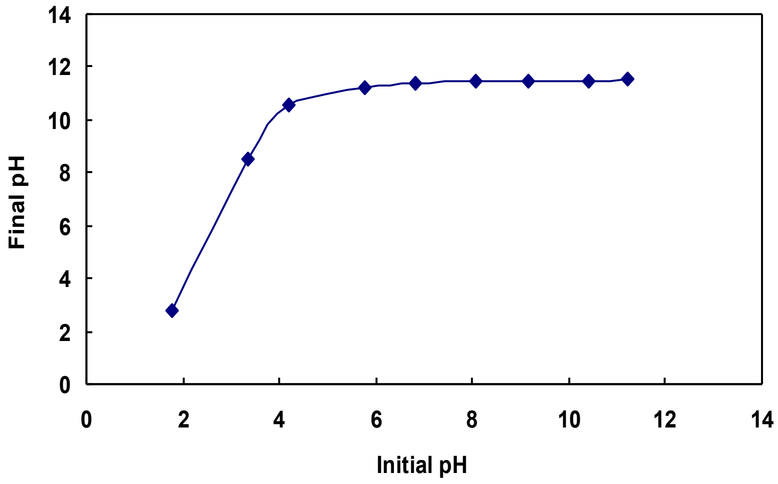

Figure 9. Effect of initial pH on the final pH (t_{EC} = 5min, C. D = 150A/m^2, d = 1cm , [NaCl] = 10g/l , A = 4.4×10 $^{-4}$ m^2,[Congo red] = 50ppm, V_S= 50ml).

Determination of iron consumption

In EC process, anode oxidizes and generates iron ions in solution that are Trans for iron hydroxide. The concentration of iron ions was determined by atomic adsorption system in different times of electrolysis and medium temperature. The result of Figure 10 showed that the amount of iron concentration in experimental is higher than theory amounts that calculated from Eq. 19. It is because for corrosion of iron in present of Na^+ and Cl^- ions and other reaction.

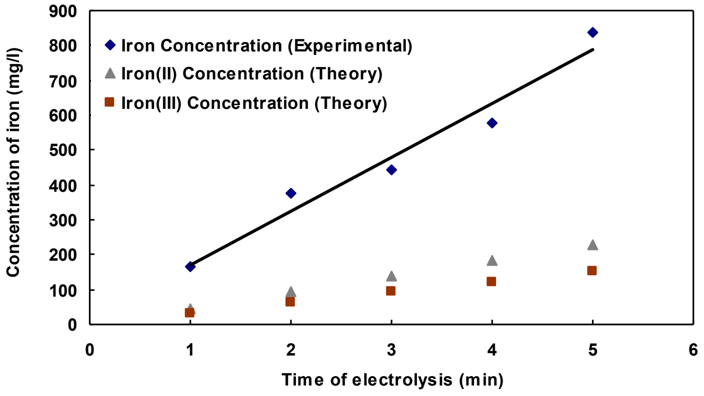

Figure 10. Effect of time of electrolysis on concentration of iron in experimental and theory in EC reactor (C.D = 150 A/m^2 , d = 1cm , [NaCl] = 10g/l , A = 4.4×10 $^{-4}$m^2 , pH $_i$= 6.7, V_S= 50ml).

In addition, the calculated iron concentrations at different temperature show in Figure 11. By increasing medium temperature, amount of generated iron particles have been increased in linear form. Probably this is due to increase rate of corrosion and later reaction. As temperature hasn't effect on the iron ions generated during electrolysis according to faraday Eq. 19.

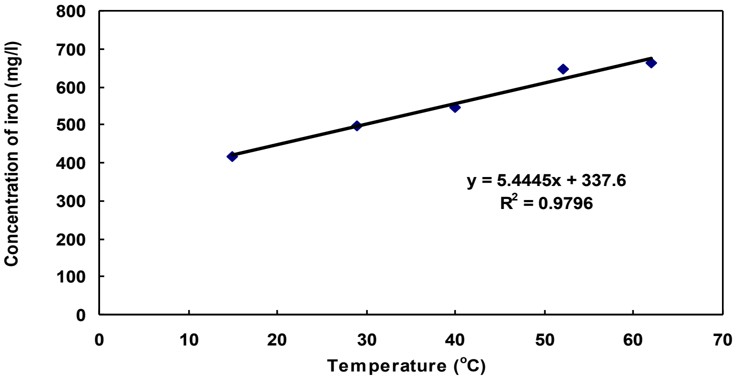

Figure 11. Effect of temperature of medium on concentration of iron in EC reactor (C.D =150A/m^2 , t_{EC} = 5min , d = 1cm , [NaCl] = 10g/l , A = 4.4×10 $^{-4}$m^2 , pH $_i$= 6.7, V_S= 100ml).

The iron concentration determinate at initial pH=6.7, after EC pH increase to 11. Also pFe in solution is between 2 to 3. Then according to Figure 12 we understand that Ferro and ferric hydroxides is stable form of iron kind in this condition in the present of oxygen and absent of oxygen respectively. They are adsorbed dye molecules and remove them in flocks form in solution with floatation or sediment or filtration.

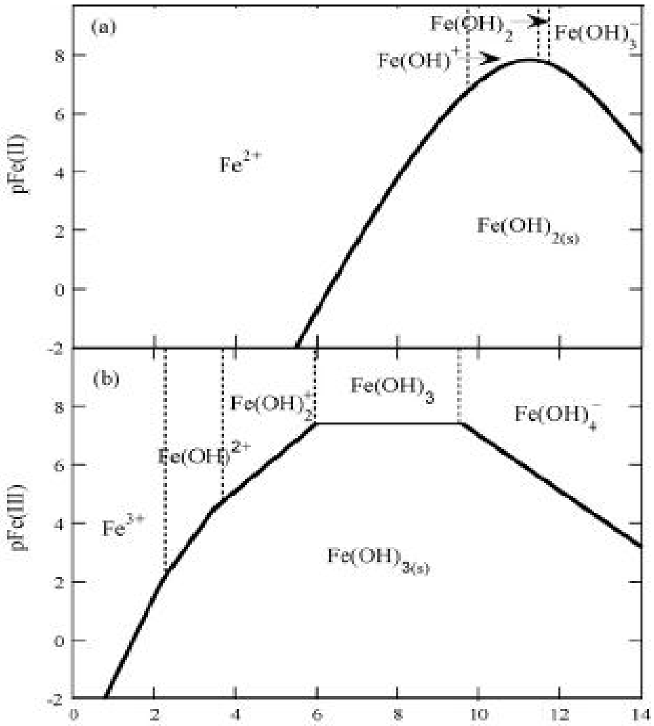

Figure 12. predominance-zone diagrams for (a) Fe(II) and (B) Fe (III) chemical species in aqueous solution.

Effect of the Temperature on the efficiency of color removal and energy consumption and Thermodynamic studies

As shown in Figure 13, raise of temperature up to 50 °C, causes an increase in removal efficiency of Congo red. The reason could be of the increase of mobility and collision of iron hydroxide flocks with dye molecules. On the other hand, at higher temperatures than 50 °C the removal efficiency is decreased. Because of the formation of unsuitable flocks or increase of the solubility of precipitates.

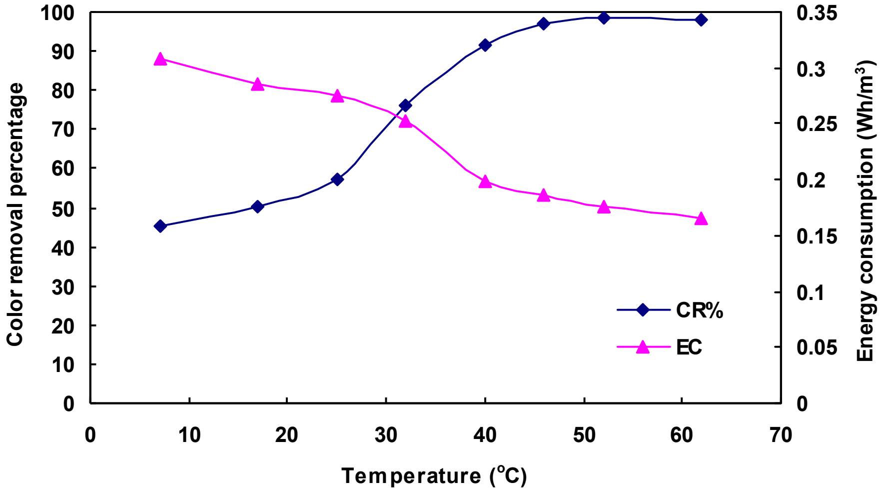

Figure 13. Effect of the Temperature on the efficiency of color removal and energy consumption (t_{EC}= 5min,C.D =150A/m^2 , d = 1cm, [NaCl] = 10g/l, A = 4.4×10 $^{-4}m^2$, [Congo red] = 50ppm, pH $_i$= 6.7, V_S= 100ml)

The amount of adsorption of Congo red on iron hydroxide flocks was measured in temperature 298–325 K. The plot of lnKd versus 1/T is shown in Figure 14. The values of ΔH° and ΔS° of Congo red adsorption were calculated by fitting the experimental data to Eq. (14) as shown in Figure 14. The values of ΔGo were obtained by using Eq. (15).

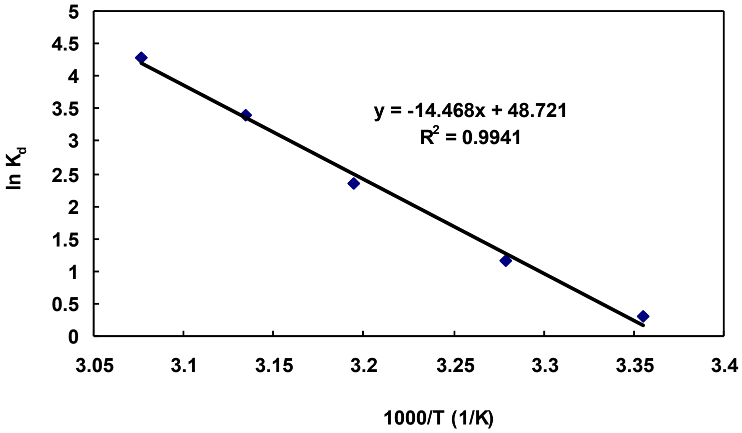

Figure 14. Plot of ln k_d versus 1/T for estimation of thermodynamic parameters. (t_{EC} = 5min,C.D=150A/m^2 , d = 1cm, [NaCl] = 10g/l, A = 4.4×10 $^{-4}m^2$, [Congo red] = 50ppm, pH $_i$= 6.7, V_S= 100ml).

The thermodynamic parameters for the adsorption of Congo red on iron hydroxide flocks are given in Table 2. As seen that the adsorption process is spontaneous with the negative values of ΔG°. The standard enthalpy change (ΔH°) for the adsorption of Congo red on iron hydroxide flocks is positive indicating that the process is endothermic in nature. The positive value of ΔS° shows increased disorder at the solid–solution interface during the adsorption of dye.

Table 2. Plot of ln k_d versus 1/T for estimation of thermodynamic parameters (t_{EC} = 5min, C.D =150A/m^2 , d = 1cm, [NaCl] = 10g/l, A = 4.4×10 $^{-4}$$m^2$, [Congo Red] = 50ppm, pH $_i$= 6.7, V_S= 100ml).

		ΔG (kJ/mol)				
ΔH (kJ/mol)	ΔS (J/mol)	298K	305K	313K	319K	325K
120.28	405.06	0.75	2.96	6.11	9.03	11.58

Congo red removal kinetics by the electrocoagulation process

The overall electrocoagulation process in Congo red removal kinetics is described by a macro-kinetics model. This model provides preliminary data for evaluating the reaction rate constants. The kinetic rate equation for representing the removal rate in Congo red concentration from the aqueous solution is described by the following mth order reaction kinetics:

$$dC/dt=-kC^m \tag{20}$$

Where *C* represents the Congo red concentration, *m* is the order of reaction, *k* is the reaction rate constant, and *t* is the time. For a first-order reaction, the above Eq. (20) becomes:

$$\ln(C_0/C_t)=k1_t \tag{21}$$

The slope of the plot of ln C_0/C_t versus time gives the value of the rate constant k_1, min^{-1}. Here, C_0 is the initial concentration in milligrams per liter, C_t is the concentration value in milligrams per liter at time *t*, and t is the time. For a second-order reaction, the above Eq. (20) becomes:

$$1/C_t-1/C_0=k_2t \tag{22}$$

The slope of the plot of ($1/C_t-1/C_0$) versus time gives the value of the rate constant k_2, 1/(mol. min). The conformity between experimental data and the model values was evaluated by the correlation values (r^2). As can be seen in Table 3, the r^2 value for the first-order model was relatively higher than that for the second-order model.

Table 3. Kinetic rate constants with first-order and second-order models for Congo red removal.

First-order model		Second-order model	
$k_1 \times 10^3$ (min)$^{-1}$	r^2	$k_2 \times 10^3$ (l/(molmin))	r^2
367	0.955	26	0.797

The first-order kinetic model as can be seen in Figure 15 which fits well with the observed data of the electrocoagulation process. It is very important to note that very fast Congo red dye removal took place at a short electrolysis time; this is considered a great advantage of using the electrocoagulation process.

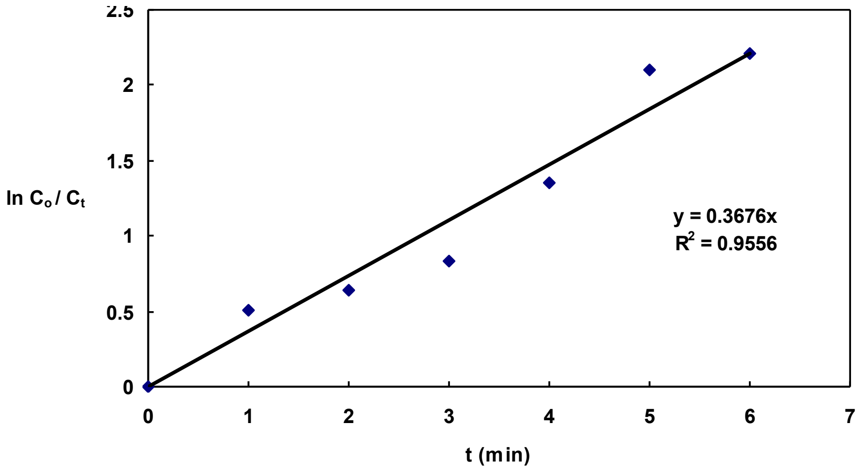

Figure 15. plot of the first-order equation for the removal kinetics of Congo red (C.D = 150 A/m^2 , d= 1cm, [NaCl] = 10g/l, A = 4.4×10 $^{-4}$m^2, [Congo red] = 50ppm, pH $_i$= 6.7, V$_S$= 50ml)

Adsorption isotherms

Critical analysis of the electrocoagulation of organic pollutants reveals that there are two separate processes taking place, i.e.

- Electrochemical process through which the metal flocks are generated.
- Physico-chemical process through which the effluents are adsorbed on the surface of the flocks [31].

The pollutant is adsorbed at the surface of the flocks generated during electrocoagulation, thus the removal of pollutant is similar to conventional adsorption except the generation of coagulants. The $Fe(OH)_n(s)$ complexes formed remains in the aqueous stream as a gelatinous suspension. These gelatinous charged hydroxo cationic complexes can effectively remove pollutants by adsorption to produce charge neutralization, by complexation, by electrostatic attraction and by enmeshment in a precipitate [32]. $Fe(OH)_2$ and $Fe(OH)_3$ is dominant species according to predominance-zone diagrams for Fe(II) and Fe(III) chemical species in aqueous solution in condition absence of oxygen and presence of oxygen respectively. A solubility diagram for Fe(II) and Fe(III) in water is presented in Fig. 12 [17]. The objective of this study is to systematically examine adsorption isotherms of $Fe(OH)_2$ and $Fe(OH)_3$ flocks for removal of Congo red from wastewater.

The iron ions consumption determinated and the amount of flocks generated can be estimated stoichiometrically. Since the amount of coagulant can be estimated for a given time for iron hydroxide (II) and (III), the pc

adsorp

the va

Congo

The v

been s

proces

$C_e/q_e =$

Where

amount of adsorbed adsorbate per unit weight of adsorbent and unadsorbed adsorbate concentration in solution at equilibrium, respectively. The constant K_L (l/g) is the Langmuir equilibrium constant and the K_L/a_L gives the theoretical monolayer saturation capacity, Q_0. Therefore, a plot of C_e/q_e versus C_e gives a straight line of slope a_L/K_L and intercepts $1/K_L$. The essential features of the Langmuir isotherm can be expressed in terms of a dimensionless constant called separation factor (R_L, also called equilibrium parameter)

ollowing equation

(24)

initial adsorbent

) is the Langmuir

rgy of adsorption.

the shape of the

avorable ($R_L > 1$),

(0 < R_L < 1) or irreversible ($R_L = 0$).

The model simulations along with experimental observations are shown in Figure 16.

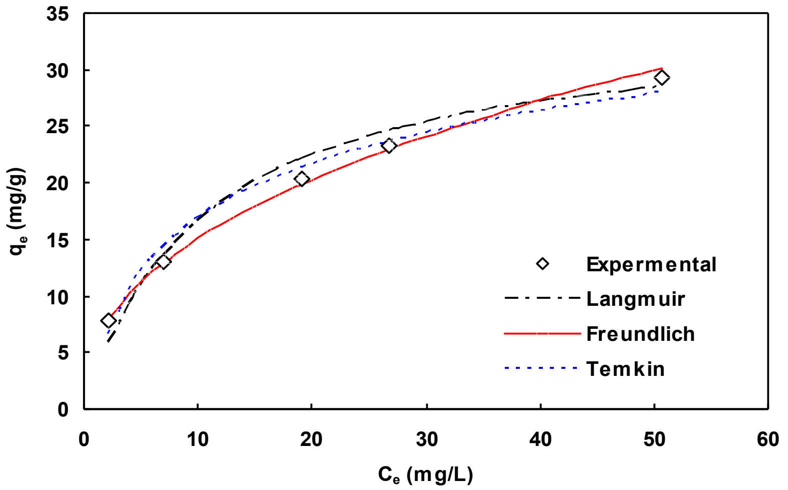

Figure 16. Equilibrium isotherms of Congo red adsorplot on iron hydroxid adsorbent (C.D = 150 A/m^2, t = 4 min, d = 1cm, [NaCl] = 10g/L, A = 4.4×10^{-4}m^2, [Congo red] = 50ppm, pH = 6.7, V_S= 50ml).

Table 4. Langmuir, Freundlich, Temkin, BET isotherm constant for Congo Red adsorption with iron (II) hydroxide flocks adsorbent.

Langmuir					Freundlich			Temkin		
K_L	a_L	Q_0	R_L	R^2	K_F	N	R^2	B	A	R^2
(L/g)	(L/mg)	(mg/g)			(mg$^{11/n}$L$^{1/n}$g^{1})	(g/L)			(L/g)	
3.28	0.092	34.48	0.518- 0.118	0.983	5.641	2.339	0.998	6.821	1.187	0.978

For a Langmuir-type adsorption process, the isotherm shape can be classified by a dimensionless constant separation factor (R_L), given by Eq. (24). It was observed that the value of R_L in the range 0-1 (Table 4 and 5) confirms the favorable uptake of the Congo red process.

Table 5. Langmuir, Freundlich, Temkin, BET isotherm constant for Congo Red adsorption with iron (III) hydroxide flocks adsorbent.

Langmuir					Freundlich			Temkin		
K_L	a_L	Q_0	R_L	R^2	K_F	N	R^2	B	A	R^2
(L/g)	(L/mg)	(mg/g)			(mg$^{11/n}$L$^{1/n}$g^{1})	(g/L)			(L/g)	
2.85	0.092	30.67	0.518- 0.118	0.983	5.021	2.339	0.998	6.071	1.187	0.978

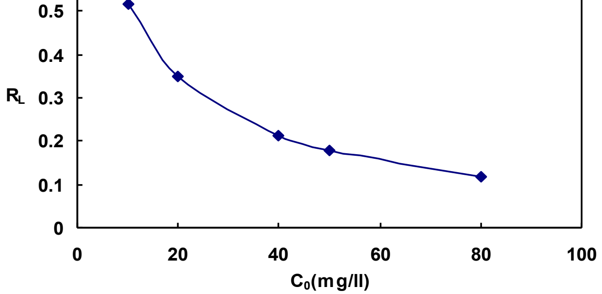

plot of separation factor versus initial Congo red concentration with iron hydroxid adsorbent (C.D = 150 min, d=1cm, [NaCl] = 10g/l, A= 4.4×10 $^{-4}$m^2, [Congo red] = 50ppm, pH $_i$= 6.7, Vs= 50ml).

The calculated R_L values at different initial Congo red concentrations are shown in Figure 17. Also lower R_L values at higher initial Congo red concentrations showed that adsorption was more favorable at higher concentration. The degree of favorability tended toward zero (the completely ideal irreversible case) rather than unity (which represents a completely reversible case). The Freundlich isotherm is an empirical model that relates the adsorption intensity of the sorbent towards adsorbent. The isotherm is adopted to describe reversible adsorption and not restricted to monolayer formation. The mathematical expression of the Freundlich model is:

$$q_e = K_F\, C_e^{\ 1/n} \qquad (25)$$

Where K_F and 1/n are the constants which give adsorption capacity and adsorption intensity, respectively. A linear form of the Freundlich model can be written as follows:

$$\log q_e = \log K_F + (1/n) \log C_e \qquad (26)$$

Plot of log q_e versus log C_e gives a straight line with slope K_F and intercept 1/n.

A basic assumption of Temkin isotherm is that the heat of sorption of all the molecules or ions in the layer decreases linearly with coverage owing to sorbate–sorbate interactions.

The Temkin isotherm has been used in the following form:

$$q_e = (RT/b) \ln A + (RT/b) \ln C_e \qquad (27)$$

$$RT/b = B \qquad (28)$$

Where *A* and *B* are Temkin constant. *A* plot of Q_e versus lnC_e enables to determine the constants *A* and *B*. The model simulation is shown in Figure 16. Table 2 shows the calculated values of Langmuir and Freundlich and Temkin model's parameters. Based on the correlation coefficient (r^2) for two adsorbent ($Fe(OH)_2$ and $Fe(OH)_3$) may be present in solution shown in Table 4 and 5, the adsorption isotherm with iron hydroxide flocks can be better described by the Freundlich equation. Also, in all cases the Freundlich equation represents a better fit of experimental data than the Langmuir and Temkin.

Conclusion

Electrocoagulation was used to remove color from dye solutions containing Congo red. The effect of various operational parameters on color removal efficiency was investigated and optimized. The decolorization of the reactive dye using iron sacrificial anode was affected by the current density, electrolysis time, the amount of NaCl, interelectrode distance, initial dye concentration, initial pH and temperature. Concentration of iron in cell in different time and temperature determined. The result showed that $Fe(OH)_2$ or $Fe(OH)_3$ is dominant spices in condition absence of oxygen and presence of oxygen respectively, can be present in aqueous solution thus the pollutant is adsorbed at the surface of the flocks generated during electrocoagulation. Then the removal of pollutant is similar to conventional adsorption except the generation of coagulants. The electrocoagulation has been modeled using adsorption isotherm models and observed the equilibrium data fit well with Freundlich adsorption isotherm model. The predictions of Freundlich adsorption isotherm model are in very good agreement to the experimental data. Our experiment results indicate that the kinetics of the Congo red can be described by the first-order model. The thermodynamic parameters, such as ΔH^o, ΔS^o and ΔG^o, were also determined and evaluated. Adsorption process is spontaneous with the negative values of ΔG^o. The standard enthalpy change (ΔH^o) for the adsorption of Congo red on iron hydroxide flocks is positive indicating that the process is endothermic in nature. The positive value of ΔS^o shows increased disorder at the solid–solution interface during the adsorption of dye.

Acknowledgements

The authors thank the University of Zanjan, Iran for financial and other supports.

References

[1] G. Annadurai, R. S. Juang, D. J. Lee, *J. Hazard. Mater.*, B92, 263 (2002).

[2] Y.C. Wong, Y. S. Szeto, W. H. Cheung, G. McKay, *Process Biochem*., 39, 693 (2004).

[3] R. Sivaraj , C. Namasivayam, K. Kadirvelu, *Waste Manage*. (Oxford)., 21, 105 (2001).

[4] M. T. Kennedy, J. M. Morgan, L. K. Benefield, A. F. McFadden, *Proceedings of the 47th Ind. Waste Conference*, West Lafayette, IN, Lewis Pub, Chelsea, MF, 727-741 (1992).

[5] T. Robinson, B. Chandran, P. Nigam, *Water Res*., 36, 2824 (2002).

[6] A. Pala, E. Tokat, *Water Res*., 36, 2920 (2002).

[7] S. F. Kang, H. M. Chang, *Water Res*., 36, 215 (1997).

[8] M. Perez, F. Torrades, X. Domenech, J. Peral, *Water Res*., 36, 2703 (2002).

[9] W. Chu, S. M. Tsui, *Water Res*., 36, 3350 (2002).

[10] A. Aleboyeh, Y. Moussa, H. Aleboyeh, *Dyes Pigm*., 66, 129 (2005).

[11] A. Aleboyeh, H. Aleboyeh, Y. Moussa, *Dyes Pigm*., 57, 67 (2003).

[12] N. Daneshvar, A. Aleboyeh, A. R. Khataee, *Chemosphere*, 59, 761 (2004).

[13] N. Daneshvar, D. Salari, A. R. Khataee, *J. Photochem. Photobiol*., A, 157, 111 (2003).

[14] N. Daneshvar, D. Salari, A. R. Khataee, *J. Photochem. Photobiol*., A, 162, 317 (2004).

[15] C. Hachem, F. Bocquillon, O. Zahraa, M. Bouchy, *Dyes Pigm*., 49, 125 (2001).

[16] M. V. B. Zanoni, J. Sene, M. A. Anderson, *J. Photochem. Photobiol.*, A, 157, 55 (2003).

[17] A. C. Martinez-Huitle, E. Brillas, Appl. Catal., B, 87, 105 (2009).

[18] N. Daneshvar, A. R. Khataee, N. Djafarzadeh, *J. Hazard. Mater.*, B137, 1788 (2006).

[19] M. Yousuf, A. Mollah, R. Schennach, J. R. Parga, D. L. Cocke, *J. Hazard. Mater.*, B84, 29 (2001).

[20] M. Kobya, O. T. Can, M. Bayramoglu, M. Sozbir, *Sep. Purif. Technol.*, 37, 117 (2004).

[21] M. Kobya, O. T. Can, M. Bayramoglu, *J. Hazard. Mater*., B100, 163 (2003).

[22] M. Kobya, O. T. Can, M. Bayramoglu, *Ind. Eng. Chem. Res.*, 42, 3391 (2003).

[23] N. Daneshvar, H. Ashassi-Sorkhabi, A. Tizpar, *Sep. Purif. Technol.*, 31, 153 (2003).

[24] N. Daneshvar, H. Ashassi-Sorkhabi, M. B. Kasiri, *J. Hazard. Mater.,* B112, 55 (2004).

[25] D. Xu, X. L. Tan, C. L. Chen, X. K. Wang, *Appl. Clay Sci.*, 41, 37 (2008).

[26] A. S. Ozcan, A. J. Ozcan, *Colloid Interface Sci.*, 276, 39 (2004).

[27] V. Vimonses, S. Lei, B. Jin, C. Chow, C. P. Saint, *Applied Clay Science.*, 43, 465 (2009).

[28] M. Y. A. Mollah, P. Morkovsky, J. A. G. Gomes, M. Kesmez, J. Parga, D. L. Cocke, *J. Hazard. Mater.*, B114 , 199 (2004).

[29] G. Chen, *Sep. Purif. Technol.*, 38, 11 (2004).

[30] N. Daneshvar, A. Oladegaragoze, N. Djafarzadeh, *J. Hazard. Mater.*, B129, 116 (2006).

[31] M. Y. A. Mollah, R. Schennach, J. R. Parga, D. L. Cocke, *J. Hazard. Mater.*, B84, 29 (2001).

[32] G. Crini, H. N. Peindy, F. Gimbert, C. Robert, *Separ. Purif. Technol.*, 53, 97 (2007).

[33] I. D. Mall, V. C. Srivastava, G. V. A. Kumar, I. M. Mishra, *Colloids Surf.*, A, 278, 175 (2006).